

Λ CDM IS CONSISTENT WITH SPARC RADIAL ACCELERATION RELATION

B.W. KELLER¹ AND J. W. WADSLEY

Department of Physics and Astronomy, McMaster University, Hamilton, Ontario, L8S 4M1, Canada

¹kellerbw@mcmaster.ca

ABSTRACT

Recent analysis (McGaugh et al. 2016) of the SPARC galaxy sample found a surprisingly tight relation between the radial acceleration inferred from the rotation curves, and the acceleration due to the baryonic components of the disc. It has been suggested that this relation may be evidence for new physics, beyond Λ CDM. In this letter we show that 32 galaxies from the MUGS2 match the SPARC acceleration relation. These cosmological simulations of star forming, rotationally supported discs were simulated with a WMAP3 Λ CDM cosmology, and match the SPARC acceleration relation with less scatter than the observational data. These results show that this acceleration relation is a consequence of dissipative collapse of baryons, rather than being evidence for exotic dark-sector physics or new dynamical laws.

Keywords: gravitation — galaxies: evolution — galaxies: kinematics and dynamics — dark matter

1. INTRODUCTION

For nearly a century, observations of kinematics in galaxies and clusters of galaxies have found large velocities inconsistent with the luminous matter within them. Even when thorough, comprehensive surveys of the baryonic mass within galaxies and clusters have been performed, most of the matter has been found to be missing. Zwicky (1937) presented observations of galaxy velocity dispersions in the Coma cluster, and proposed that the bulk of that cluster’s mass was some sort of dark matter (DM). Later, the groundbreaking observations of Rubin & Ford (1970) showed that this dark matter was also ubiquitous within disc galaxies like our own. Today, there is a wealth of evidence for cold dark matter, not just from galaxy kinematics, but from the formation of large-scale structure (Blumenthal et al. 1984), the cosmic microwave background power spectrum (Planck Collaboration et al. 2014), and the primordial abundances of elements after Big Bang Nucleosynthesis (Walker et al. 1991). Dark matter is now part of the standard cosmology, Λ CDM, in which most of the matter in our universe is in fact dark. Despite this, we still do not know the actual form that dark matter particles take. Both direct detection experiments and searches for dark matter annihilation have failed to conclusively observe these particles (Aprile et al. 2012), and as such, alternative explanations for the kinematics of galaxies have been proposed.

The Spitzer Photometry & Accurate Rotation Curves (SPARC) sample, presented in Lelli et al. (2016a) is a

new set of observations and derived mass models for a large number of rotation-dominated galaxies. By using $3.6\mu\text{m}$ observations, the stellar mass can be estimated with great accuracy. The stellar mass is complemented with 21cm observations of HI to get a measure of the gas mass within the disc. The recent paper by McGaugh et al. (2016) analyzed this sample, and determined a relation between the observed radial acceleration determined from the rotation curve (g_{obs}), and the acceleration induced by the baryons observed in the disc (g_{bar}). McGaugh et al. (2016) found that for large values of g_{bar} , $g_{\text{obs}} \sim g_{\text{bar}}$, while for values of $g_{\text{bar}} \lesssim 10^{-10} \text{m s}^{-2}$, the observed acceleration begins to rapidly outstrip the acceleration one would expect from the observed baryons. They find that the relation between g_{bar} and g_{obs} is well fit by:

$$g_{\text{obs}} = \frac{g_{\text{bar}}}{1 - \exp(-\sqrt{g_{\text{bar}}/g_{\ddagger}})}, \quad (1)$$

where $g_{\ddagger} = 1.20 \pm 0.26 \times 10^{-10} \text{ms}^{-2}$. In addition to the simple functional form, McGaugh et al. (2016) find a surprisingly low scatter in this relation, with residuals normally distributed with $\sigma = 0.11$ dex. The authors noted that this is the same functional form as the Modified Newtonian Dynamics (MOND) (Milgrom 1983) acceleration law, which attempts to explain galaxy rotation curves without DM.

A correlation between the total acceleration seen in disc galaxies and the acceleration due only to baryons has been known for some time Sancisi (2004); McGaugh (2004). Until recently, this has primarily been exam-

ined through the Mass-Discrepancy Acceleration Relation (MDAR): g_{bar} vs. M_{tot}/M_{bar} . [McGaugh et al. \(2016\)](#) directly probes a more fundamental relation, the Radial Acceleration Relation (RAR), with number of improvements that reduce the observational uncertainties.

In discussing these results, [McGaugh et al. \(2016\)](#) offer three possible explanations for the tight relation.

1. The end point of galaxy formation with conventional (baryonic?) physics.
2. New dark sector physics coupling dark matter and baryons
3. New dynamical laws (such as MOND Tensor-Vector-Scalar Gravity (TeVeS) ([Bekenstein 2004](#)), etc.)

This is not the first set of observations that appear to be in discordance with Λ CDM. N-body simulations of halo formation have found DM halos follow a universal, “cuspy” density profile ([Navarro et al. 1996](#)). Yet observations of dwarf galaxies in the local universe find flat, “cored” central densities (the “cusp-core problem”, [Walker & Peñarrubia 2011](#)). Meanwhile, DM-only simulations were finding that the local group should contain thousands of dwarfs, in contrast to the dozens actually observed (the “missing satellites problem” [Klypin et al. 1999](#)). Many of these halos are large enough that suppression of star formation by reionization could not explain their absence from the observations (the “too big to fail” problem [Boylan-Kolchin et al. 2011](#)).

A common feature in each of these conflicts is the comparison of observations to simulations of galaxy formation that rely purely on N-body, DM-only simulations. We now know that the impact of baryonic physics, chief among them the feedback from massive stars and black holes, can have a dramatic effect on the star formation history (e.g. [Keller et al. 2015](#)) and density profile of galaxies ([Mashchenko et al. 2006](#)). Multiple studies ([Pontzen & Governato 2012](#); [Sawala et al. 2016](#), etc) have found these problems disappear when galaxies are simulated with gas dynamics, along with reasonable models for star formation, radiative cooling, and stellar feedback. This is what constitutes a modern theory of galaxy formation, the first of the three options offered to explain the RAR. Galaxies are formed through the gravitational collapse of collisional particles (gas) into a rotationally supported disc. Conservation of angular momentum, combined with star formation and feedback within that disc, leads to the observed scaling relations and galaxy properties we see today. Whether this can also reproduce the RAR has been yet to be demonstrated.

In this letter, we show that the apparent tension between models of galaxy formation in Λ CDM and the SPARC observations also evaporates when the collisional collapse of baryons is taken into account. We find that the $g_{obs} - g_{bar}$ relation for a set of pre-existing cosmological galaxy simulations, evolved in a conventional Λ CDM cosmology, matches the SPARC acceleration relation, with even tighter scatter than the observed sample.

2. THE MUGS2 SAMPLE

The McMaster Unbiased Galaxy Simulations 2 (MUGS2) sample is an unbiased, statistically representative set of 18 cosmological zoom-in simulations of L^* disc galaxies. These galaxies were simulated in a WMAP3 Λ CDM cosmology, with parameters $H_0 = 73 \text{ km s}^{-1} \text{ Mpc}^{-1}$, $\Omega_M = 0.24$, $\Omega_{bar} = 0.04$, $\Omega_\Lambda = 0.76$, and $\sigma_8 = 0.76$. The MUGS2 $z = 0$ halo masses range from $3.7 \times 10^{11} M_\odot$ to $2.2 \times 10^{12} M_\odot$, with disc masses ranging from $1.8 \times 10^{10} M_\odot$ to $2.7 \times 10^{11} M_\odot$. For more details on the creation of the MUGS2 initial conditions, see the original MUGS paper, [Stinson et al. \(2010\)](#). For more information on the simulations themselves, see [Keller et al. \(2015, 2016\)](#).

MUGS2 was simulated using the modern smoothed particle hydrodynamics code GASOLINE ([Wadsley et al. 2004](#); [Keller et al. 2014](#)). The simulations used metal line radiative cooling ([Shen et al. 2010](#)), as well as a simple Schmidt law for star formation. What sets MUGS2 apart from the original MUGS, aside from improved hydrodynamics, is the use of a physically motivated, first principles model for treating feedback from supernovae. (SNe). Originally presented in [Keller et al. \(2014\)](#), the superbubble model captures the effects of thermal conduction and evaporation between a hot, SNe heated bubble and a surrounding shell of cold, swept-up interstellar medium (ISM). This model was derived to allow unresolved superbubbles to radiatively cool at realistic rates, with no free parameters, while automatically capturing the effects of clustered SNe.

In addition to the central spirals, we also include a number of dwarf companions from the MUGS2 sample. As with [McGaugh et al. \(2016\)](#), we exclude galaxies that are experiencing significant tidal interactions. [Joshi et al. \(2016\)](#) showed that tidal interactions on infalling galaxies can occasionally be seen out to 3 virial radii, we select galaxies between 3 to 5 virial radii from the central spiral. We exclude halos beyond 5 virial radii because our zoom-in simulations do not contain gas particles at these distances. In order to limit the effects of poor resolution, and to ensure that each radial bin contains sufficient baryonic resolution, we select only galaxies that contain 100 or more star particles. This gives us an additional 14 galaxies at $z = 0$, for a total of 32

Galaxy	M_*	M_{gas}	M_{vir}
$g15807_3$	1.66×10^7	1.52×10^8	1.74×10^{10}
$g8893_1$	2.14×10^7	1.06×10^7	1.10×10^{10}
$g1536_2$	2.62×10^7	1.03×10^8	8.36×10^9
$g3021_1$	3.24×10^7	3.93×10^7	2.49×10^{10}
$g4145_3$	4.04×10^7	9.55×10^7	2.83×10^{10}
$g7124_1$	4.76×10^7	2.83×10^8	3.54×10^{10}
$g27491_1$	6.66×10^7	4.22×10^8	2.53×10^{10}
$g1536_1$	1.19×10^8	3.75×10^8	5.29×10^{10}
$g4145_2$	1.76×10^8	8.40×10^8	4.83×10^{10}
$g15807_2$	3.04×10^8	1.09×10^9	5.50×10^{10}
$g4145_1$	3.93×10^8	5.29×10^8	1.30×10^{11}
$g15807_1$	7.54×10^8	1.68×10^9	8.17×10^{10}
$g4720_1$	1.03×10^9	1.36×10^9	9.70×10^{10}
$g22437_1$	1.94×10^9	8.22×10^8	1.53×10^{11}
$g7124_0$	5.22×10^9	4.97×10^{10}	3.66×10^{11}
$g8893_0$	7.36×10^9	9.10×10^{10}	5.80×10^{11}
$g5664_0$	9.44×10^9	7.29×10^{10}	4.77×10^{11}
$g21647_0$	1.18×10^{10}	1.01×10^{11}	7.44×10^{11}
$g422_0$	1.51×10^{10}	1.24×10^{11}	7.62×10^{11}
$g28547_0$	1.59×10^{10}	1.67×10^{11}	9.85×10^{11}
$g1536_0$	1.86×10^{10}	1.04×10^{11}	6.49×10^{11}
$g24334_0$	2.55×10^{10}	1.53×10^{11}	1.02×10^{12}
$g3021_0$	3.63×10^{10}	1.51×10^{11}	9.78×10^{11}
$g19195_0$	7.15×10^{10}	9.34×10^{10}	1.01×10^{12}
$g22437_0$	9.03×10^{10}	7.31×10^{10}	8.52×10^{11}
$g22795_0$	1.06×10^{11}	4.55×10^{10}	8.52×10^{11}
$g15784_0$	1.30×10^{11}	1.14×10^{11}	1.31×10^{12}
$g4720_0$	1.42×10^{11}	5.51×10^{10}	1.02×10^{12}
$g4145_0$	1.50×10^{11}	8.09×10^{10}	1.19×10^{12}
$g25271_0$	1.56×10^{11}	7.87×10^{10}	1.25×10^{12}
$g27491_0$	1.88×10^{11}	2.08×10^{11}	2.14×10^{12}
$g15807_0$	2.14×10^{11}	1.75×10^{11}	2.03×10^{12}

Table 1. Redshift 0 properties of our simulated galaxies. All masses are in solar masses. Subscript 0 denotes the central galaxy.

galaxies. The stellar, gas, and total virial masses for each of our galaxies is shown in table 1.

2.1. Calculating Accelerations from MUGS2

In order to compare to the SPARC sample, we located the central halos using the AMIGA halo finder [Knollmann & Knebe \(2009\)](#). We center the halos using the shrinking sphere method described in [Power et al. \(2003\)](#). Next, in order to measure rotation curves of the galaxies face-on, we calculate the net angular momentum vector of all gas within 10 kpc of the center of the disk, and rotate our simulations such that this vector is orthogonal to the x-y plane. Accelerations were mea-

sured in 100 circular annuli 300 pc thick. For dwarfs, we use 15 600 pc-thick annuli, as the dwarfs have much smaller scale lengths, and to avoid issues from poor sampling of the dark matter or baryon particles within the dwarfs. Accelerations were then calculated using a direct N-body summation on all of the particles in the halo on those particles within the annulus. Only the in-plane component of the acceleration was used, to better follow [McGaugh et al. \(2016\)](#). For g_{obs} (the observed acceleration), all particles (gas, stars, and DM) within the simulation were used. To calculate g_{bar} , we simply calculate the contributions from stars and gas, g_* and g_{gas} , so that $g_{\text{bar}} = g_* + g_{\text{gas}}$. For each of g_* and g_{gas} , we use a direct summation only on those particles (stars and gas respectively). This process of direct summation to calculate gravity is equivalent to the numerical solution to Poisson’s equation used in ([McGaugh et al. 2016](#)). The mass model in SPARC ([Lelli et al. 2016a](#)) included stellar masses estimated from 3.6 μm near infrared observations, and gas masses estimated using 21 cm observations of HI. These HI masses were converted to total gas masses using the simple equation $M_{\text{gas}} = 1.33M_{\text{HI}}$. Rather than using the total gas mass from our simulations, we follow the HI-based estimate from SPARC by calculating accelerations due to gas using $1.33M_{\text{HI}}$, rather than M_{gas} . This is especially important near the outskirts of the galaxy, where the contribution to the baryonic mass from ionized gas in the ISM and circumgalactic medium is most significant. The HI fraction is calculated using the radiative cooling code within GASOLINE, which relies on tabulated equilibrium cooling rates from CLOUDY ([Ferland et al. 2013](#)).

3. RESULTS

3.1. $z=0$ Acceleration Relation

The MUGS2 sample gives us 2100 acceleration data points, just over 3/4 the sample size of [McGaugh et al. \(2016\)](#). Figure 1 shows the $g_{\text{obs}} - g_{\text{bar}}$ relation for the MUGS2 sample, compared both to the pure baryonic acceleration and the RAR. It is clear these simulated galaxies follow the [McGaugh et al. \(2016\)](#) relation *extremely* well. As can be seen from the inset residual distribution, our simulated galaxies follow the SPARC RAR even more tightly than the actual observational data. The scatter in our results, with $\sigma = 0.06$ dex, is consistent with the [McGaugh et al. \(2016\)](#) estimates. They decomposed their scatter of 0.11 dex into different sources, and when all of the observational uncertainties are removed, the remaining intrinsic scatter gives a variance of $\sigma = 0.06$ dex, very close to the value presented here. A reduced χ^2 statistic of the SPARC relation fit to the $z = 0$ MUGS2 data finds a very good fit, with $\chi^2_{\nu} = 1.25$. These simulation data are fit by equation 1

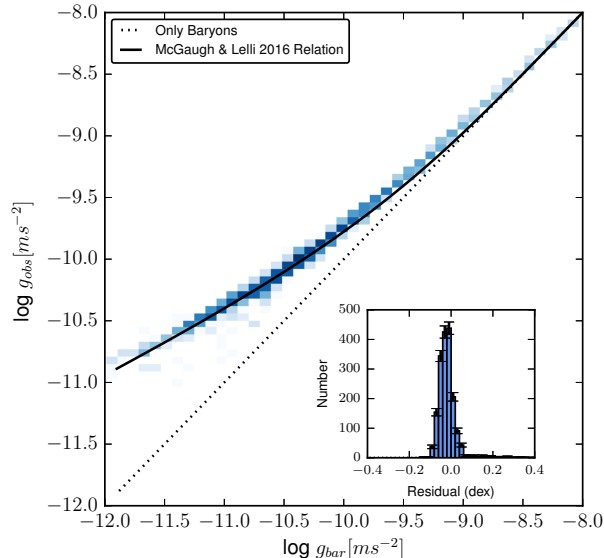


Figure 1. Total acceleration (g_{obs}) vs acceleration due to baryons (g_{bar}) from 2100 data points in the $z = 0$ MUGS2 sample, shown in the blue 2-dimensional histogram. The dotted black curve shows the 1:1 relation expected if the acceleration was due to baryons alone (without dark matter), while the solid line shows the relation presented in [McGaugh et al. \(2016\)](#). A Gaussian distribution fitted to these residuals finds a variance of $\sigma = 0.06$ dex, significantly lower than the 0.11 dex found by [McGaugh et al. \(2016\)](#).

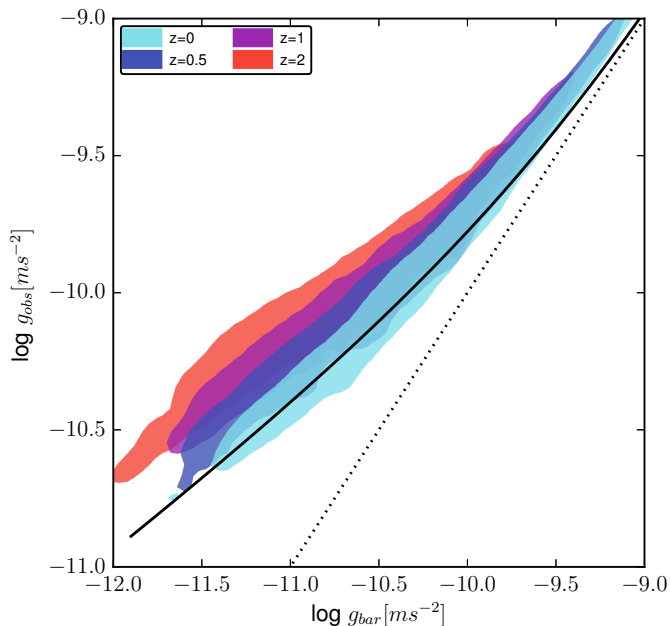


Figure 2. The simulated $g_{obs} - g_{bar}$ relation is not constant with redshift. As this figure shows, at higher redshift the low g_{bar} slope is much shallower than at $z = 0$. This shows that for high redshift galaxies, their discs can be depleted of baryons compared with $z = 0$. We have focused on the low g_{bar} end of the relation here, where the changes are most significant.

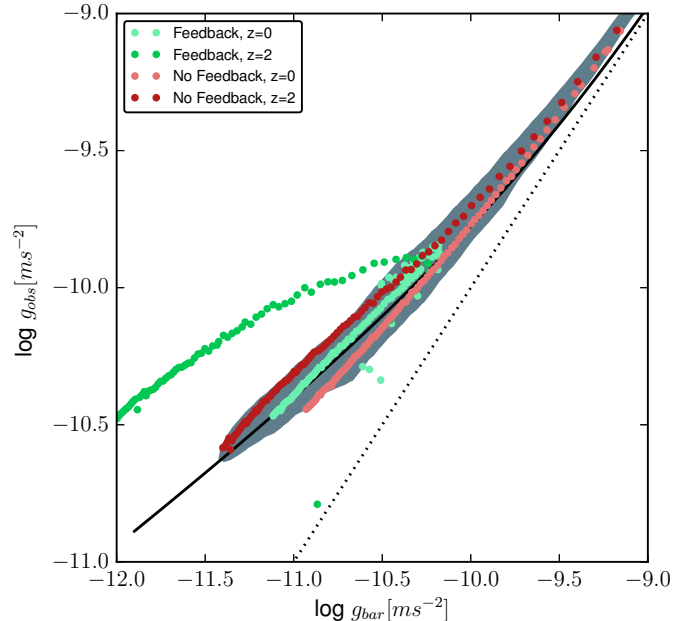


Figure 3. The evolution seen in figure 2 is primarily driven by feedback. This can be seen when looking at the same galaxy with and without feedback. Without feedback, the baryon fraction within the disc increases slightly from $z = 0$ to $z = 2$, but still roughly follows the RAR. At $z = 2$, strong outflows in the galaxy expel most of the baryons from the disc, flattening the acceleration relation. This effect is sensitive to the frequent merger-driven starbursts at high redshift, which can drive bursty outflows.

at least as well as the original SPARC data.

3.2. Feedback & the Evolution of the Acceleration Relation

If the SPARC acceleration relation is in fact due to new physics, it would be surprising if the relation did not hold at all redshifts. This would not be the case if the relation was simply a consequence of galaxy evolution. In figure 2 we show that the acceleration relation in the MUGS2 sample actually shows significant redshift dependence, and only settles to the equation 1 relation near $z=0$. For these data points, we scaled the thickness of the annuli by the cosmic scale factor a , so that $\delta r = 300/(1+z)$ pc. This scaling ensures we are sampling primarily from the stellar disc, and not well beyond it. Omitting this scaling has little effect on these results, save for extending the points to very low values of g_{bar} and removing points from the high g_{bar} end. This evolution is a consequence of the huge impact that stellar feedback has on galaxies at $z \sim 2$. [Keller et al. \(2015\)](#) showed that SNe drive hot outflows from high redshift galaxies with mass loadings of $\dot{M}_{out}/\dot{M}_* \sim 10$. This leads to discs at high redshift with baryon fractions depleted relative to those at low redshift. This feedback effect is clear when a single galaxy, g1536, is compared to the same galaxy simulated without SNe feedback. As

figure 3 shows, the redshift trend is nearly nonexistent without SNe feedback. Even at $z = 2$, the galaxy without feedback falls within the scatter of the SPARC observations, and within the scatter of the $z = 0$ MUGS2 relation. This tells us that we need not invoke feedback processes to explain the $z = 0$ SPARC RAR. Simple dissipational collapse of gas is sufficient to produce a similar relation. The evolution as a function of redshift is therefore dominated primarily by the stronger effect of feedback at higher redshift.

4. DISCUSSION

This paper is the first work to show that the RAR’s acceleration scale and tight scatter, as reported by [McGaugh et al. \(2016\)](#), can be arise from fully self-consistent hydrodynamical simulations.

Efforts have been made in the past to explain related acceleration relations (the MDAR, the Baryonic Tully Fisher (BTFR) ([McGaugh et al. 2000](#)), etc.) with analytic arguments ([van den Bosch & Dalcanton 2000](#); [Kaplighat & Turner 2002](#)), existing scaling relations ([Di Cintio & Lelli 2016](#)), or hydrodynamical simulations ([Santos-Santos et al. 2016](#)). Analytic studies have found that the MOND-like scaling relations can arise as a consequence of exponential discs living within an an NFW halo ([van den Bosch & Dalcanton 2000](#)). [van den Bosch & Dalcanton \(2000\)](#) showed that this can explain not only Tully-Fisher relation’s relatively tight scaling over a large range of masses and surface densities ([McGaugh & de Blok 1998](#)), but even explain the appearance of a characteristic acceleration in disk galaxy rotation curves ([McGaugh 1999](#)).

Subsequent studies have suggested that an even harder constraint for Λ CDM to match is the tight scatter in the MDAR ([Wu & Kroupa 2015](#)) or the RAR ([Milgrom 2016](#)). A semi-empirical model recently published by [Di Cintio & Lelli \(2016\)](#) showed that both the BTFR and the MDAR can arise as a result of galaxies that follow a handful of scaling relations both for the baryonic content of the galaxy, as well as the dark matter halo it resided within. Both their model matches to the MDAR and the BTFR did show slightly higher scatter than the [Lelli et al. \(2016b\)](#) observations (0.17 vs. 0.11 (0.06 intrinsic) dex), which they suggest may be a result of the BTFR’s sensitivity to measuring radius.

The BTFR and MDAR were also examined using galaxies from the MaGICC ([Stinson et al. 2013](#)) and CLUES ([Gottloeber et al. 2010](#)) simulations by [Santos-Santos et al. \(2016\)](#). Their results also showed similar scatter to the MDAR reported in [McGaugh](#)

(2014), with a scatter of $\sigma \sim 0.3$ dex.¹ This is significantly higher than the intrinsic scatter of 0.06 dex reported in [McGaugh et al. \(2016\)](#). This may be due to the use of a sample composed of simulations run using different subgrid physics prescriptions, which will naturally differ from one another. While matching the scatter of previous observations, which suffered from much higher observational uncertainties, matching both the fitting function and small intrinsic scatter of [McGaugh et al. \(2016\)](#) has never been done prior to this study.

Concurrently with the work presented here, [Ludlow et al. \(2016\)](#) presented a study using simulations from the EAGLE ([Schaye et al. 2015](#)) and APOSTLE ([Sawala et al. 2016](#)) projects. EAGLE and APOSTLE use a common set of subgrid physics. They found their simulations were fit well by the [McGaugh et al. \(2016\)](#) functional form of the RAR with $g_{\dagger} = 3 \times 10^{-10} \text{ ms}^{-2}$ (well outside the uncertainties reported in [McGaugh et al. \(2016\)](#) for the value of g_{\dagger}). They also found that the $z=0$ relation is only somewhat sensitive to the subgrid physics model (as we have found as well). The fact that their g_{\dagger} is larger than ours means EAGLE galaxies are somewhat baryon-depleted compared to ours. This, coupled with the lack of redshift evolution, suggests that the EAGLE feedback model drives stronger outflows at low redshift compared to the superbubble model used in MUGS2.

The EAGLE subgrid physics model is complex, and involves a number of different purely numerical parameters that were tuned to reproduce the observed stellar mass to halo mass relation (SMHMR) and size-mass relation, the details of which can be found in [Crain et al. \(2015\)](#). MUGS2 instead used a well-constrained, physically motivated model for SN feedback ([Keller et al. 2014](#)), with no free parameters beyond the energy available per supernovae, and which captures the effects of thermal evaporation that are ignored in EAGLE. This allows us to better capture the real variation that occurs in the efficiency of outflows over cosmic time ([Keller et al. 2015](#); [Muratov et al. 2015](#)). Perhaps the clearest conclusion that can be drawn from the results of this paper and those of [Ludlow et al. \(2016\)](#) is that the scatter in the RAR will be fairly small regardless of the details of baryonic process like cooling, star formation, and feedback. However, the actual value of g_{\dagger} is sensitive to these details, and the RAR may therefore be a useful new tool for constraining subgrid physics in galaxy simulations.

¹ While this number is not reported in [McGaugh \(2014\)](#), we have confirmed this value with Dr. McGaugh in private communication.

5. CONCLUSION

We have shown here that the SPARC RAR can be produced by conventional galaxy formation in a Λ CDM universe. While we have used a pre-existing set of simulations, MUGS2, we expect a larger sample designed to match SPARC should find similar results. Neither the particular functional form (equation 1) nor the small scatter about this relation requires anything beyond the dissipational collapse of baryons in a DM halo. We predict the fit observed at $z = 0$ will not hold at all redshifts: vigorous feedback at high redshift acts to scour protogalaxies of their baryons, reducing the baryon fraction of the disc, flattening the $g_{obs} - g_{bar}$ relation. Stellar feedback is an essential process if we are to produce realistic galaxies. In order for a single RAR to hold at all redshifts, feedback efficiencies would have to be so low as to produce galaxies with stellar masses and bulge fractions in conflict with the observed SMHMR, and the observed kinematics of local galaxies. If one wished to use equation 1 to fit galaxies at all epochs, g_{\dagger} would need to have a significant redshift dependence. If, on the other

hand, high redshift observations of the $g_{obs} - g_{bar}$ relation found no evolution in shape, or a steeper slope at low g_{bar} , this would in fact constitute a serious disagreement with Λ CDM, as it would be difficult to produce the observed low cosmic star formation efficiency without strong outflows removing baryons from high redshift discs.

As figure 3 shows, the $z = 0$ SPARC relation is *not* a result of stellar feedback. While feedback does change the relationship at high redshift, its general form is reproduced by simple gas collapse and radiative cooling. This is one of the few apparent problems in Λ CDM that *doesn't* require feedback for its resolution!

ACKNOWLEDGEMENTS

We thank Hugh Couchman, Stacy McGaugh, and Laura Parker for valuable discussion and suggestions. The simulations used here were performed on SCINET, part of ComputeCanada. We appreciate these computing allocations. We also thank NSERC for funding support.

REFERENCES

- Aprile, E., Alfonsi, M., Arisaka, K., et al. 2012, Physical Review Letters, 109, 181301
- Bekenstein, J. D. 2004, Phys. Rev. D, 70, 083509
- Blumenthal, G. R., Faber, S. M., Primack, J. R., & Rees, M. J. 1984, Nature, 311, 517
- Boylan-Kolchin, M., Bullock, J. S., & Kaplinghat, M. 2011, MNRAS, 415, L40
- Crain, R. A., Schaye, J., Bower, R. G., et al. 2015, MNRAS, 450, 1937
- Di Cintio, A., & Lelli, F. 2016, MNRAS, 456, L127
- Ferland, G. J., Porter, R. L., van Hoof, P. A. M., et al. 2013, RMxAA, 49, 137
- Gottloeber, S., Hoffman, Y., & Yepes, G. 2010, ArXiv e-prints, arXiv:1005.2687
- Joshi, G. D., Parker, L. C., & Wadsley, J. 2016, MNRAS, 462, 761
- Kaplinghat, M., & Turner, M. 2002, ApJ, 569, L19
- Keller, B. W., Wadsley, J., Benincasa, S. M., & Couchman, H. M. P. 2014, MNRAS, 442, 3013
- Keller, B. W., Wadsley, J., & Couchman, H. M. P. 2015, MNRAS, 453, 3499
- . 2016, MNRAS, arXiv:1604.08244
- Klypin, A., Kravtsov, A. V., Valenzuela, O., & Prada, F. 1999, ApJ, 522, 82
- Knollmann, S. R., & Knebe, A. 2009, ApJS, 182, 608
- Lelli, F., McGaugh, S. S., & Schombert, J. M. 2016a, ArXiv e-prints, arXiv:1606.09251
- . 2016b, ApJ, 816, L14
- Ludlow, A. D., Benitez-Llambay, A., Schaller, M., et al. 2016, ArXiv e-prints, arXiv:1610.07663
- Mashchenko, S., Couchman, H. M. P., & Wadsley, J. 2006, Nature, 442, 539
- McGaugh, S. 1999, in Astronomical Society of the Pacific Conference Series, Vol. 182, Galaxy Dynamics - A Rutgers Symposium, ed. D. R. Merritt, M. Valluri, & J. A. Sellwood
- McGaugh, S. 2014, Galaxies, 2, 601
- McGaugh, S., Lelli, F., & Schombert, J. 2016, ArXiv e-prints, arXiv:1609.05917
- McGaugh, S. S. 2004, ApJ, 609, 652
- McGaugh, S. S., & de Blok, W. J. G. 1998, ApJ, 499, 41
- McGaugh, S. S., Schombert, J. M., Bothun, G. D., & de Blok, W. J. G. 2000, ApJ, 533, L99
- Milgrom, M. 1983, ApJ, 270, 371
- . 2016, ArXiv e-prints, arXiv:1609.06642
- Muratov, A. L., Kereš, D., Faucher-Giguère, C.-A., et al. 2015, MNRAS, 454, 2691
- Navarro, J. F., Frenk, C. S., & White, S. D. M. 1996, ApJ, 462, 563
- Planck Collaboration, Ade, P. A. R., Aghanim, N., et al. 2014, A&A, 571, A16
- Pontzen, A., & Governato, F. 2012, MNRAS, 421, 3464
- Power, C., Navarro, J. F., Jenkins, A., et al. 2003, MNRAS, 338, 14
- Rubin, V. C., & Ford, Jr., W. K. 1970, ApJ, 159, 379
- Sancisi, R. 2004, in IAU Symposium, Vol. 220, Dark Matter in Galaxies, ed. S. Ryder, D. Pisano, M. Walker, & K. Freeman, 233
- Santos-Santos, I. M., Brook, C. B., Stinson, G., et al. 2016, MNRAS, 455, 476
- Sawala, T., Frenk, C. S., Fattahi, A., et al. 2016, MNRAS, 457, 1931
- Schaye, J., Crain, R. A., Bower, R. G., et al. 2015, MNRAS, 446, 521
- Shen, S., Wadsley, J., & Stinson, G. 2010, MNRAS, 407, 1581
- Stinson, G. S., Bailin, J., Couchman, H., et al. 2010, MNRAS, 408, 812
- Stinson, G. S., Brook, C., Macciò, A. V., et al. 2013, MNRAS, 428, 129
- van den Bosch, F. C., & Dalcanton, J. J. 2000, ApJ, 534, 146
- Wadsley, J. W., Stadel, J., & Quinn, T. 2004, New Astronomy, 9, 137
- Walker, M. G., & Peñarrubia, J. 2011, ApJ, 742, 20

Walker, T. P., Steigman, G., Kang, H.-S., Schramm, D. M., &
Olive, K. A. 1991, *ApJ*, 376, 51
Wu, X., & Kroupa, P. 2015, *MNRAS*, 446, 330

Zwicky, F. 1937, *ApJ*, 86, 217